Eighth velocity of light

S. C. Bloch
Physics Department, University of South Florida, Tampa, Florida 33620
(Received 13 February 1976; revised 22 September 1976)

In dispersive media the phase velocity, group velocity, energy velocity, signal velocity, relativistic velocity constant, and ratio-of-units velocity are usually not useful concepts for wave packets. The centrovelocity has been suggested as a measure which overcomes many of the objections to the first six. We describe yet another, based on the cross-correlation of the original and received wave packets, which is shown to be useful in time-of-flight measurements in weakly and strongly dispersive media; absorption and amplification are readily accommodated. Applications for specific examples of wave packets in magnetoplasmas are presented.

I. INTRODUCTION

The subject of wave propagation in dispersive media has attracted the attention of scientists, mathematicians, and engineers for many years. Applications today are abundant, from solid state physics to water waves and sound waves to lasers and high-speed pulse communication through rocket exhausts, interplanetary plasmas, and fiber-optic light guides.

Dispersive propagation has been a recurrent theme in the pages of this Journal. In a previous paper[1] we presented a heuristic calculation of pulse compression in a dispersive system, which is the conceptual inverse of the usual discussion of pulse spreading,[2-5] and we stressed the unity of the physically different phenomena of dispersive propagation and diffraction as forms of generalized diffraction in terms of the Fourier transform. For completeness here we mention some of the earlier papers listed in Ref. 1: Crawford[6-8] has reported some especially interesting acoustic effects; Merrill[9] has presented a BASIC computer program for study of dispersive pulse propagation; and a series of papers[10-13] have described experiments suitable for student use, including a backward wave system (phase velocity and group velocity in opposite directions).

In addition to these, York[14] has presented a graphical approach to dispersion; Baird[15] has discussed the very useful concept of moments of a wave packet; Prestwich[16] noted a precise definition of group velocity; Jones[17] reemphasized the mathematical analogy between diffraction and dispersive propagation; and Berry and Greenwood[18] reiterated the ubiquity of the sine wave in dispersive linear systems, as the only waveform that preserves its shape while propagating. Guillemin[19] earlier had written almost poetically of the sine wave ". . . the sinusoid was singled out as the *one* that shall forever be king and ruler. . . . *No other periodic function can claim such distinction!* . . . There is something very peculiar—yes, almost uncanny—about the sinusoidal waveform that gives it the property of remaining unaltered when another sinusoid having the same period but any amplitude and random phase is added to it. . . . No other periodic function can lay claim to this property either. . . . The sinusoid is unique in that its shape is invariant to integration or differentiation, no matter how often either operation may be repeated. . . . the sinusoid is the building block from which anything else can be constructed. . . . the sinusoid is nature's building block also." Healy and Power[20] treated the subtle problems of crossing symmetry in deriving dispersion relations for optically active media; Dean[21] noted a simple oscilloscope demonstration of group velocity; and Rader[22] called attention to the dispersive effect of absorption, a point to which we shall return later. Christy[23] reviewed the classical theory of optical dispersion, and Khan and Mahendra[24] calculated exact optical indices in the resonance region. The universality of Kramers–Kronig relations was reviewed by Holbrow and Davidon,[25] Sharnoff,[26] and Scott.[27] The subject of dispersive propagation is currently of great interest and activity,[28-36] and there are possibilities of applications in models of talandic phenomena in socio-psychological systems.[37]

It would be futile at present to argue which is the most fundamental constant of nature, but if such a debate occurred, certainly a good case could be made for the velocity of light, the study of which led to our contemporary views of the universe. There are six rather common measures of the velocity of light; Smith[38] has suggested a seventh which overcomes many limitations of the first six. The purpose of this paper is to describe yet another velocity of light which has become practical only because of modern electronic instrumentation and the availability of digital computers. Several advantages and results of applications of the eighth velocity will be presented.

The concept of the eighth velocity is not new, but it is not widely known. It is used in some advanced radars and, for mechanical waves, in certain aspects of seismology and acoustics.

II. SEVEN VELOCITIES OF LIGHT

A. The first six

Six measures of the velocity of light are well known (though often only by name): (1) phase velocity, (2) group velocity, (3) energy velocity, (4) signal velocity, (5) relativistic velocity constant, and (6) ratio-of-units velocity. The first two are perhaps the most familiar, but there are several difficulties associated with them. For example, the group velocity in a region of anomalous dispersion may change sign or exceed the velocity of light in vacuum,[5,39] and for an electron in a crystal lattice the group velocity is found by the same relationship as that for free electrons, $v_g = \hbar^{-1}\nabla_k \epsilon(k)$, obscuring the fact that there is a periodic motion like an inchworm superimposed on this average motion.[40] Russakoff[41] has clarified some of the points involved in deriving the macroscopic Maxwell equations from the microscopic equations of electrodynamics, emphasizing that physical insight must accompany the mathematical procedures of taking temporal and spatial averages.[3]

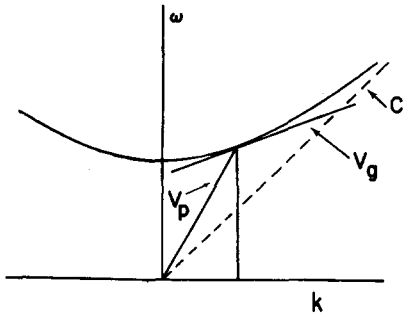

Fig. 1. Brillouin or ω-k diagram. For a monochromatic plane wave, phase velocity at frequency ω is ω/k. Group velocity is $d\omega/dk$. For the particular dispersion relation shown here, ω/k becomes infinite when $d\omega/dk$ goes to zero.

The phase velocity is only defined for a monochromatic wave; for the more interesting case of a wave packet there is no unique value for phase velocity. The group velocity, $d\omega/dk$ evaluated at k_0 (the mean value of the wave number), and the phase velocity, ω/k for a plane wave, may even be in opposite directions, as shown graphically on the Brillouin or ω-k diagrams in Figs. 1 and 2.

Smith[38] has reviewed and clarified the basic characteristics and concepts of the velocities of light; the reader is referred to his paper for detailed discussion and critical evaluation of the first six.

B. The seventh: centrovelocity

Smith[38] proposed a new definition of the velocity of light, the centrovelocity, defined by

$$v_c = \left| \nabla \left[\int_{-\infty}^{+\infty} tE^2(\mathbf{r},t)\, dt \right] \times \left[\int_{-\infty}^{+\infty} E^2(\mathbf{r},t)\, dt \right]^{-1} \right|^{-1}, \quad (1)$$

where $E(\mathbf{r},t)$ is the real amplitude of the microscopic electric field of the radiation field.[42] This velocity describes the motion of the first moment of the temporal intensity or energy distribution in a manner analogous to the center-of-mass velocity in mechanics. It is well behaved in a region of anomalous dispersion and has a close connection with the flow of energy. It provides an experimentally measurable quantity, compatible with time-of-flight methods. It is apparently useful in anisotropic media since different centrovelocities can be defined for two states of polarization in orthogonal planes or for two states of (contrarotating) circular polarization.

Since the centrovelocity depends on the distribution of energy in a pulse, it suffers from some of the objections expressed for the energy velocity and the signal velocity; i.e., there may actually not be any energy arriving at the time specified by the centrovelocity, at which time half of the energy has already arrived and half is still expected. This is analogous to the fact that, if the earth were blown to pieces by a thermonuclear device, the center of mass would still serenely orbit the sun.

Secondly, the operational definition, Eq. (1), is carried out in the time domain and involves a difficult computational procedure on a computer, which would be required for any real-world problem.

III. THE CORRELATION VELOCITY

A. Concept of cross-correlation

We digress momentarily to review the process of cross-correlation, which is basic to what follows. The idea of pattern-matching by sliding one object over another has its origin in antiquity. Perhaps some persons still obtain correlations by sliding chart recordings or oscilloscope photos. This idea can be made quantitatively precise by defining the cross correlation for periodic functions as

$$R_{1,2}(\tau) = T^{-1} \int_0^T E_1(t)E_2(t+\tau)\, dt, \quad (2)$$

where T is the period of E_1 and E_2, E_1 is one waveform and $E_2(t+\tau)$ is another waveform shifted by the delay time parameter τ. The maximum of the cross-correlation $R_{1,2}(\tau)$ occurs when E_2 is shifted so that it most closely matches E_1. Clearly, this idea is not restricted to functions of time, but it is applicable to any variable. If E_1 and E_2 are the same waveform, Eq. (2) yields the autocorrelation function.

The behavior of Eq. (2) can be illustrated graphically by a simple device. Suppose one takes a piece of graph paper and outlines a pulse, say, 5 units wide and one unit high with the left (earliest) edge of the pulse at, say, 7 units to the right of the origin. Then one makes a transparency of the graph and proceeds to slide the transparency in small increments across the original graph. At each increment one measures the overlap product and plots this as a function of the increment number. This process is shown in Fig. 3, and Table I contains the results. What we have described is discrete one-dimensional cross-correlation. The universal result that we have obtained is that the cross-correlation of a rectangle with a similar rectangle is a triangle with its apex located at the time delay of the leading edge of the unshifted rectangle. The cross-correlation of any other waveforms will yield other functions, but the peak will occur at the time delay. Although it is perhaps not immediately apparent, correlation is a powerful technique for discovering hidden periodicities and for digging signals out of noise. Correlation is not limited to periodic functions, of course, but aperiodic functions are probably not of importance for the problem faced here.

The process of shift, multiply, and add that we have described is time-consuming even on a digital computer. Thanks to the fast Fourier transform (FFT) it is now possible to carry out high-speed correlation (and convolution) by means of the Wiener–Khintchine theorem, which relates the cross-correlation to the inverse Fourier transform of the cross spectral density,

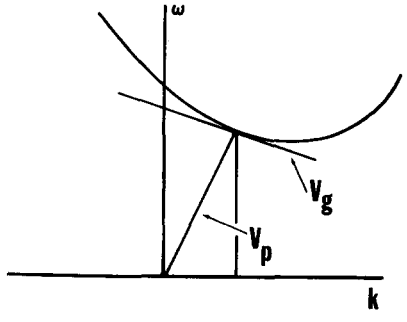

Fig. 2. Brillouin diagram for a dispersion relation with a backward wave. Phase velocity ω/k is positive and group velocity $d\omega/dk$ is negative.

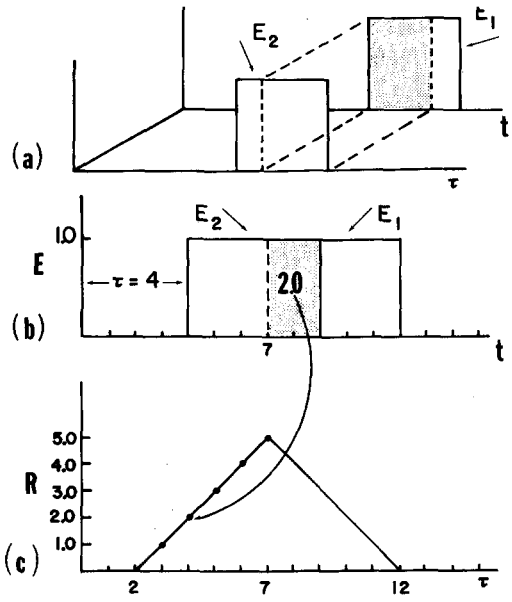

Fig. 3. Correlation process with two similar rectangular waveforms. (a) Original waveform replica (E_2) is time-shifted across propagated waveform (E_1). (b) Overlap product = 2 for $\tau = 4$. (c) Overlap product plotted as a function of time shift. (See Table I for data.)

$$R_{1,2}(\tau) = (2\pi)^{-1} \int_{-\infty}^{+\infty} A_1(\omega) A_2^*(\omega) e^{i\omega\tau}\, d\omega. \quad (3)$$

For Eq. (3) one uses the FFT on E_1 and E_2 to find A_1 and A_2; then one forms the product $A_1 A_2^*$ and applies the inverse FFT to this cross spectral density. Use of Eq. (3) in lieu of Eq. (2) results in great savings in computer time.

B. Correlation and velocity of light

We can view the preceding example as if the original pulse were time-shifted across the transmitted pulse at the receiving site. Since the cross-correlation peaks at the value of τ corresponding to the leading edge of the pulse that has traversed a vacuum distance d, it is reasonable to define the correlation velocity as

$$v_{\text{cor}} = d/\tau_{\max}, \quad (4)$$

where $\tau_{\max}$ is the time delay at which $R_{1,2}(\tau)$ achieves its maximum value.

We have explicitly defined v_{cor} as the ratio of the propagation distance to the time delay; we shall investigate its properties for dispersive propagation and we shall show that it yields usable results in highly dispersive and absorptive situations in which the original pulse becomes so distorted

Table I. $R_{1,2}(\tau)$ for two similar rectangular pulses [data from Fig. 3(b), plotted in Fig. 3(c)].

τ	Overlap product	τ	Overlap product
0	0	8	4
1	0	9	3
2	0	10	2
3	1	11	1
4	2	12	0
5	3	13	0
6	4	14	0
7	5	15	0

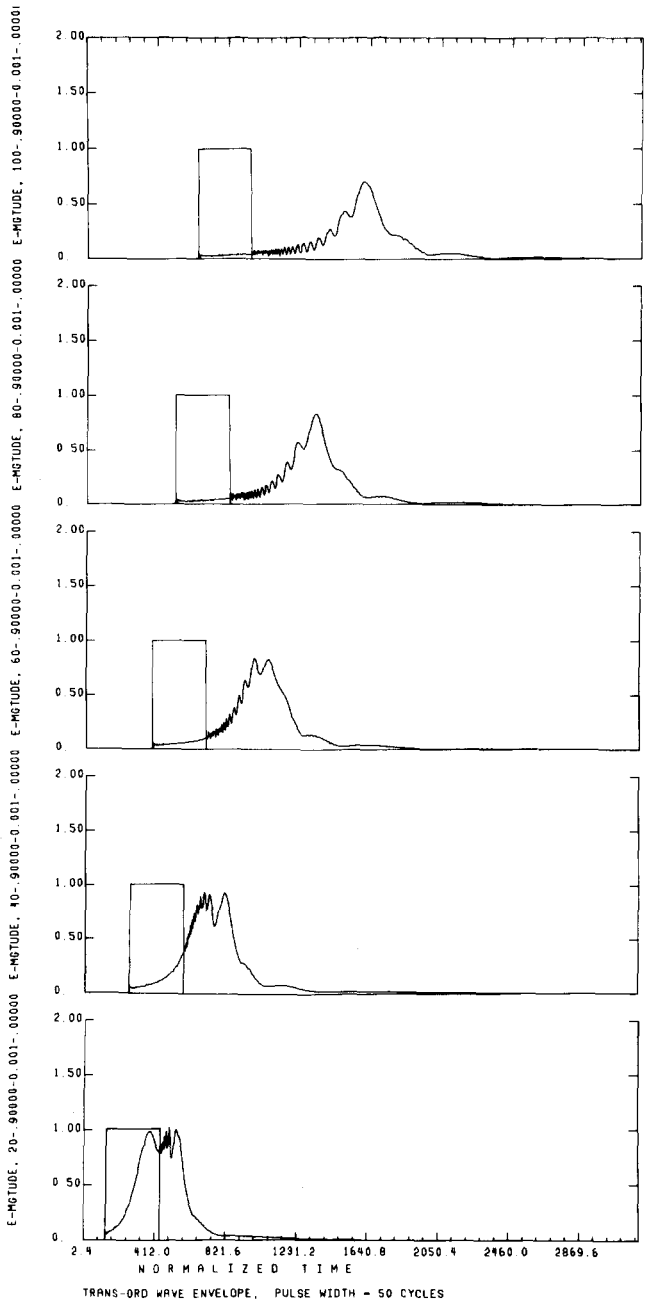

Fig. 4. Dispersion and absorption of a rectangular pulse envelope containing 50 cycles of a sine wave; propagation in the ordinary mode. Vacuum propagation is shown in rectangular outline. $\omega_p/\omega_0 = 0.9$ and $\nu/\omega_0 = 0.001$. From bottom to top, $d/\lambda_0 = 20$, 40, 60, 80, and 100 vacuum-equivalent wavelengths of the central frequency of the original pulse. (See Table II for data.)

that it is not readily recognizable. Our results will be computed in the absence of noise, an idealized situation, but the use of v_{cor} is not restricted to such a case. In fact, v_{cor} is relatively immune to the natural statistical fluctuations of the medium and random signals and noise. Suppose that all of the noise and fluctuations can be represented by a random electric field $E_r(t)$. Then the spectrum of the received wave form is given by

$$A_1'(\omega) = \int_{-\infty}^{+\infty} [E_1(t) + E_r(t)] e^{-i\omega t}\, dt \quad (5)$$

or

$$A_1'(\omega) = A_1(\omega) + A_r(\omega). \quad (6)$$

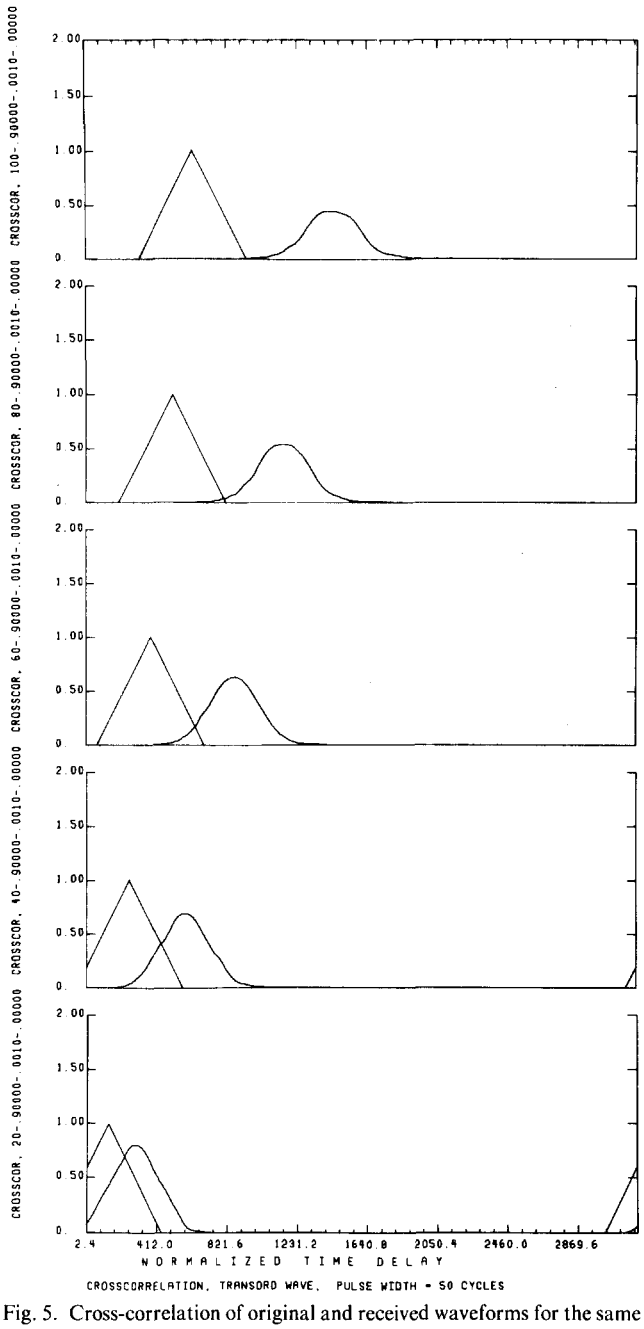

Fig. 5. Cross-correlation of original and received waveforms for the same conditions as in Fig. 4. Vacuum propagation is shown in triangular outline. (See Table II for data.)

After substitution of Eq. (6) into Eq. (3) one obtains

$$R_{1,2}'(\tau) = (2\pi)^{-1} \int_{-\infty}^{+\infty} [A_1(\omega) + A_r(\omega)] A_2^*(\omega) e^{i\omega\tau}\, d\omega \quad (7)$$

$$= R_{1,2}(\tau) + R_{r,2}(\tau). \quad (8)$$

In Eq. (8) the cross-correlation of the random field with the original pulse will ordinarily be vanishingly small compared with $R_{1,2}(\tau)$, so that measurements may be carried out in the presence of a signal-to-noise ratio that otherwise might be intolerable.

C. Applications of correlation velocity

We have already shown[36] that, for Faraday rotation of pulsed electromagnetic waves in a magnetoplasma, the cross-correlation of the original and received signals can be more useful than the electric fields themselves in measuring the rotation of the plane of polarization of an initially linearly polarized wave packet. For a concrete example here we shall also choose pulses in a magnetoplasma, a dispersive, anisotropic, nonreciprocal medium with several resonances, cutoffs, and modes of propagation, and with broad-band (collisional) absorption and narrow-band (resonant) absorption. In such a medium characterized by an antisymmetric permittivity or conductivity tensor, Murphy's law can be considered to be valid until proven otherwise. It follows that, if the correlation velocity is useful in such a complex medium, it may also be useful in simpler media.

For a cold magnetoplasma governed by the Appleton-Hartree dispersion relation one may discuss wave propagation in terms of the thirteen distinct regions on the Clemmow-Mullaly-Allis diagram. For the first example we select the simplest case of propagation perpendicular to $\mathbf{B}_0$ with $\mathbf{E}$ parallel to $\mathbf{B}_0$, which is usually termed the ordinary mode. For this case the magnetic field has no effect and the dispersion relation is given by

$$k_+(\omega) = (\omega/c)\{1 - [\omega_p^2/(\omega^2 + \nu^2)] - i\nu\omega_p^2/[\omega(\omega^2 + \nu^2)]\}^{1/2}, \quad (9)$$

where $k_+(\omega)$ is the propagation factor, ω is the radian fre-

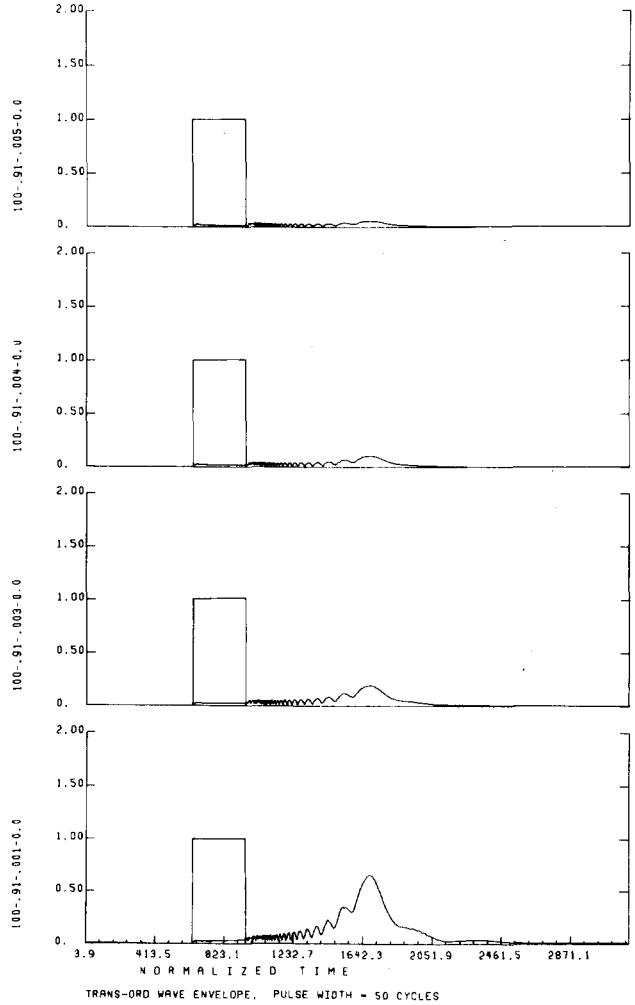

Fig. 6. Effects of collisional absorption on time evolution of ordinary wave. $d/\lambda_0 = 100$, $\omega_p/\omega_0 = 0.91$, and (from bottom to top) $\nu/\omega_0 = 0.001, 0.003, 0.004, 0.005$.

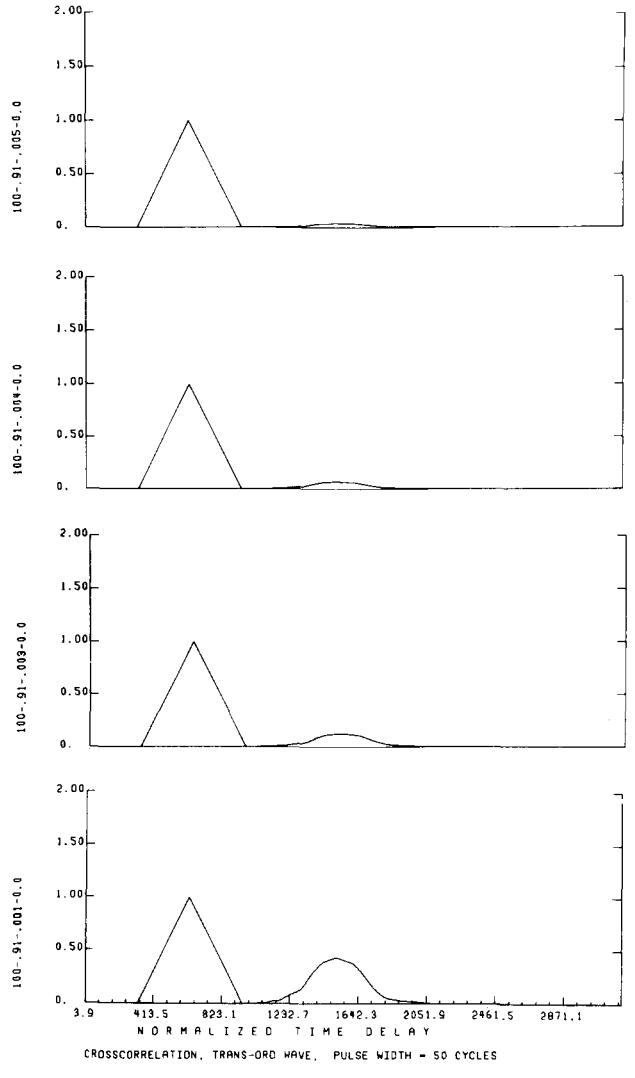

Fig. 7. Cross-correlation of original and received ordinary waves for the same conditions as in Fig. 6. Collisional absorption becomes apparent in decreased correlation and shorter time delay. From bottom to top, cross-correlation (and real time delay in $\omega_0\tau$ units) are: 0.43081 (1510.32), 0.12301 (1507.18), 0.06593 (1495.40), 0.03559 (1492.26) and for ν/ω_0 = 0.006 (not shown here), 0.01924 (1489.11).

quency, c is the velocity of light in vacuum, $\omega_p{}^2 = ne^2/m\epsilon_0$ is the square of the electron plasma frequency, $i = \sqrt{-1}$, and ν is the effective electron–heavy particle collision frequency for momentum transfer given by[43]

$$\nu = (8\pi N)\left(\frac{m}{2\pi\kappa T_e}\right)^{5/2}\int_0^\infty v^5 q_m(v) \times \exp\left(\frac{-mv^2}{2\kappa T_e}\right) dv. \quad (10)$$

The electron charge, density, mass, and velocity are given, respectively, by e, n, m, and v; ϵ_0 is the vacuum permittivity, N is the density of heavy particles, κ is Boltzmann's constant, T_e is the absolute electron temperature, and $q_m(v)$ is the collision cross section for momentum transfer.

In Fig. 4 we show the results of a computer analysis of pulse propagation in accordance with Eq. (9). The rectangle indicates the result for vacuum propagation. In all of the figures, we indicate normalized time in units of $\omega_0 t$ and normalized time delay in units of $\omega_0\tau$. The ordinate labels on all plots indicate normalized propagation length d/λ_0, plasma frequency ω_p/ω_0, collision frequency ν/ω_0, and cyclotron frequency ω_c/ω_0. In the preceding, ω_0 and λ_0 refer to the central frequency of the original pulse and the corresponding wavelength, $\omega_c = eB_0/m$, is the electron cyclotron frequency, and B_0 is the static magnetic field. Thus propagation length is expressed in vacuum-equivalent wavelengths of the central frequency of the original pulse, and the plasma parameters are normalized to the central frequency of the original pulse. For example, the ordinate label on the lowest plot in Fig. 4 indicates, respectively, normalized propagation length, plasma frequency, collision frequency, and cyclotron frequency in the sequence 20–0.90000–0.001–0.00000.

The magnetic field has been set to zero for the ordinary wave because it does not enter into the dispersion relation, Eq. (9); this dispersion relation is, in fact, the same as that for an unmagnetized plasma. In Fig. 4 we can see the pulse become progressively more distorted as it propagates farther into the magnetoplasma. The qualitative observation of distortion is confirmed by the cross-correlation of the received and original pulse plotted in Fig. 5; the peak value of the cross-correlation decreases and the spread increases. The qualitative ideas expressed earlier concerning the other measures of pulse velocity are apparent in Fig. 4, except that we have not included noise. In the real world the base line would not be zero in Fig. 4; it would obscure the leading and trailing edges of the pulse in an unpredictable manner. In contrast, the peak of the cross-correlation in Fig. 5 would be practically unaffected in position even though its magnitude might decrease slightly, depending on the signal-to-noise ratio.

In Fig. 4 the high frequencies arrive first, followed by the main body of the wave packet, and the slower, lower frequencies bring up the rear. How does one say when such a distorted wave packet has "arrived"? In Fig. 5 it is easy to determine the peak values which mark the time delays for use in Eq. (4).

In Eq. (9) there is a wave cutoff when $k_+(\omega) \to 0$ at $\omega = \omega_p$ in the absence of collisions, and this is the major cause of dispersion in this mode. In Figs. 6 and 7 we show the dispersive effect of broad-band absorption due to elastic collisions. The plasma parameters are the same as in Figs. 4 and 5, but in Figs. 6 and 7 the varying parameter is ν. For the values of parameters in this example the effect of absorption is to increase the speed of the wave packet very slightly. This is readily apparent in cross-correlation but not so obvious in the waveform itself.

In Fig. 8 we plot the waveform for propagation in the extraordinary mode, i.e., $\mathbf{k} \perp \mathbf{B}_0$ and $\mathbf{E} \perp \mathbf{B}_0$, for the same plasma parameters as in Fig. 4. We now see the effect of the magnetic field, which in our example has $\omega_c = 0.1\omega_p$. The dispersion relation for the extraordinary mode is given by

$$k_-(\omega) = (\omega/c)\{1 - \omega_p{}^2[(\omega^2 - \omega_p{}^2)(\omega^2 - \omega_p{}^2 - \omega_c{}^2) + \nu^2\omega^2][\omega^2(\omega^2 - \omega_p{}^2 - \omega_c{}^2 - \nu^2)^2 + \nu^2(2\omega^2 - \omega_p{}^2)^2]^{-1}\} - i\nu\omega_p{}^2[\omega_p{}^4 + \omega^2(\omega^2 - 2\omega_p{}^2 + \omega_c{}^2 + \nu^2)]\{\omega[\omega^2(\omega^2 - \omega_p{}^2 - \omega_c{}^2 - \nu^2)^2 + \nu^2(2\omega^2 - \omega_p{}^2)^2]\}^{-1})^{1/2}. \quad (11)$$

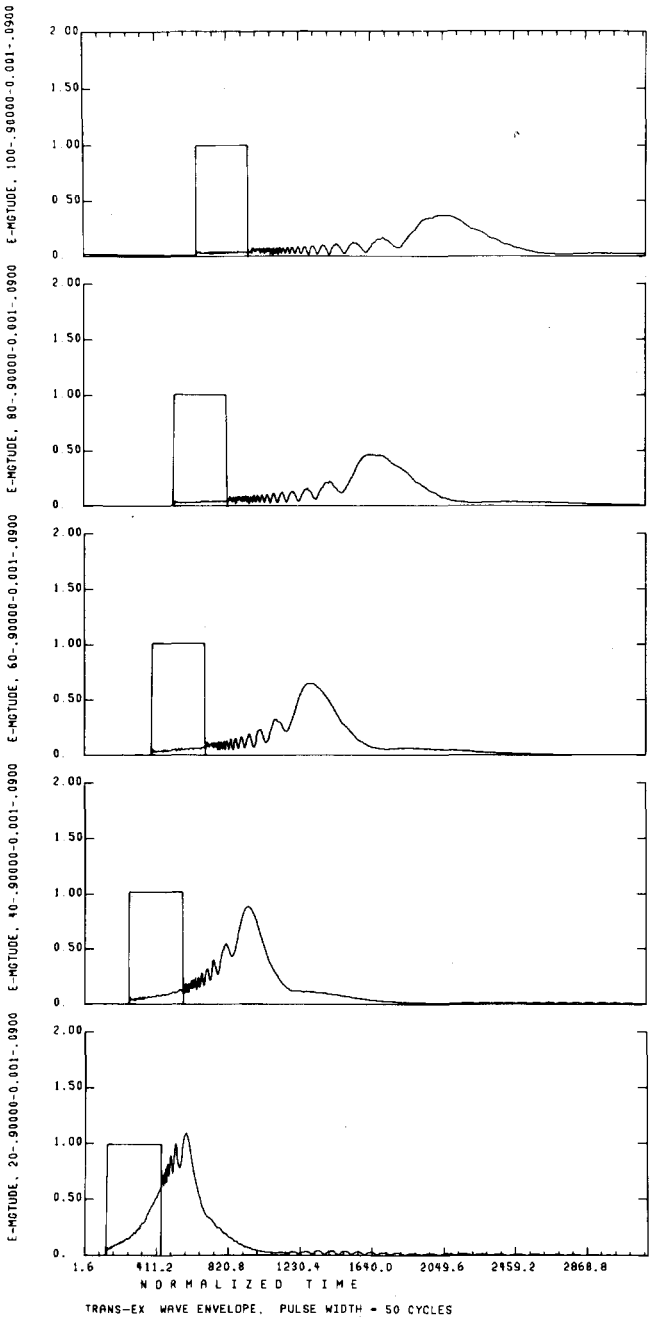

Fig. 8. Dispersion and absorption of rectangular pulse envelope for propagation in the extraordinary mode, for same parameters as in Figs. 4 and 5. (See Table II for data.)

In the absence of collisions there is a resonance when $k_- \to \infty$ at the upper hybrid frequency $\omega_{uh} = (\omega_p^2 + \omega_c^2)^{1/2}$; in addition to this resonance there are cutoffs ($k_- \to 0$) at $\omega_p^2/\omega_0^2 \pm \omega_c/\omega_0 = 1$. All contribute to dispersion. In the extraordinary mode there is a longitudinal component of the electric field as well as a transverse component. Thus the wave is, in general, elliptically polarized in the plane perpendicular to the static magnetic field. Here we confine our attention to the transverse component. In Fig. 9 we plot the cross-correlation for Fig. 8. The decorrelation of the propagating pulses is due to the absorption as well as the dispersion of the medium; the magnetic field in the extraordinary mode increases both effects.

In Figs. 4 and 8 it is difficult to say when the pulse arrives, but there is no effort in determining the peak value of the cross-correlation in Figs. 5 and 9. If noise were present in Figs. 4 and 8, it would raise the base line and obscure the lower part of the pulse, making the problem of using the waveform even more difficult. Use of the cross-correlation is not hampered by changes in the base line because we are only interested in the time when the peak occurs, not the value of the peak or the area under the curve.

In Table II we show the pertinent data from Figs. 5 and 9, for which a word of explanation is in order. Our data are contained in an array of 2^{12} points, and although the figures are plotted as the envelopes of the waveforms and cross-correlations for purposes of graphic clarity, the computations are based on samplings of each cycle of the wave. For economic reasons our printout selects only every sixteenth point of the envelope, which results in an uncertainty in the peak cross-correlation time delay of $\pm 15/4096$, or about

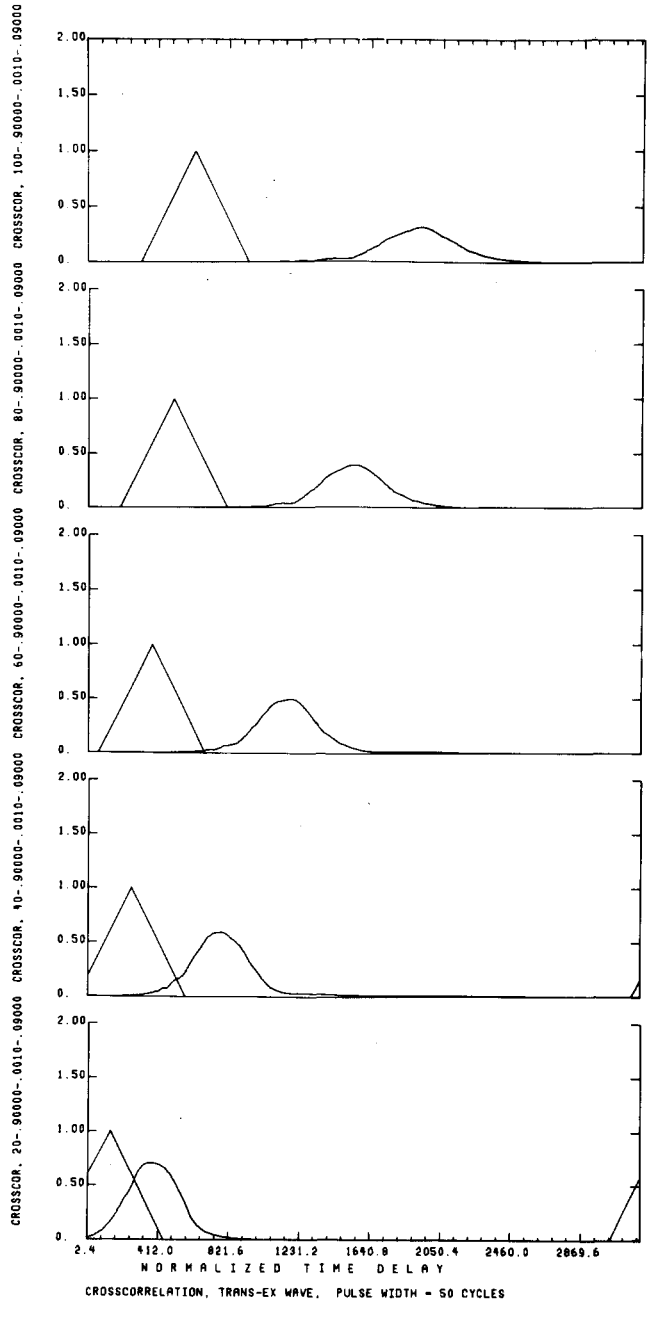

Fig. 9. Cross-correlation of original and received extraordinary wave for the same parameters as in Figs. 4, 5, and 8. (See Table II for data.)

Table II. Normalized time delay and cross-correlation for propagation perpendicular to $\mathbf{B}_0$. $\omega_p/\omega_0 = 0.9$, $\nu/\omega_0 = 0.001$, $\omega_c/\omega_0 = 0.09$, pulse width = 50 cycles.

d/λ_0	Vacuum propagation, real time $\omega_0\tau_{max}$	Ordinary wave: Plasma real time	Ordinary wave: Plasma 4096 time	Extraordinary wave: Plasma real time	Extraordinary wave: Plasma 4096 time	Ordinary wave maximum $R_{1,2}$	Extraordinary wave maximum $R_{1,2}$
20	125.66	278.03	354	363.64	463	0.80393	0.71314
40	251.33	567.84	723	773.62	985	0.69238	0.59063
60	376.99	871.01	1109	1174.96	1496	0.63114	0.49711
80	502.65	1139.61	1451	1541.74	1963	0.54149	0.39967
100	628.32	1430.21	1821	1929.72	2457	0.44887	0.31690

0.37%, and this is reducible without limit by means of a larger array and a higher resolution in the printout. In Table II, "4096 time" is computer printout time and "real time" is $\pi/4$ times "4096 time." As an example of the use of Table II, consider a microwave signal with center frequency in the X band, $\omega_0 = 2\pi \times 10^{10}$ Hz and $\lambda_0 = 2\pi c/\omega_0 = 3 \times 10^{-2}$ m. Then for $d/\lambda_0 = 100$, we have $d = 3$ m. For vacuum propagation through 3 m, $\tau_{max} = 2\pi(100)/(2\pi \times 10^{10}) = 10^{-8}$ sec. For the plasma parameters in Table II, for the ordinary wave we find $\tau_{max} = 1821\ (\pi/4)/(2\pi \times 10^{10}) = 2.28 \times 10^{-8}$ sec and for the extraordinary wave $\tau_{max} = 2457\ (\pi/4)/(2\pi \times 10^{10}) = 3.07 \times 10^{-8}$ sec. The corresponding velocities are: ordinary wave, $800c/1821$; extraordinary wave, $800c/2457$. These and other data from Table II are plotted in Fig. 10.

As a final example of propagation across the magnetic field in a highly dispersive and absorptive medium we plot, in Figs. 11 and 12, respectively, the time delay and cross-correlation for a frequency sweep through the upper hybrid resonance. Since we normalize all parameters with respect to the central frequency of the original pulse, a frequency sweep results in variation of all normalized parameters. Such a frequency sweep is common in the laboratory and in ionospheric sounding, topside and bottomside.

For propagation parallel to the static magnetic field the dispersion relation is given by

$$k_{l,r}(\omega) = (\omega/c)\{1 - \omega_p{}^2(\omega \pm \omega_c)/[\omega(\omega \pm \omega_c)^2 + \nu^2\omega] - i\nu\omega_p{}^2/[\omega(\omega \pm \omega_c)^2 + \nu^2\omega]\}^{1/2}, \quad (12)$$

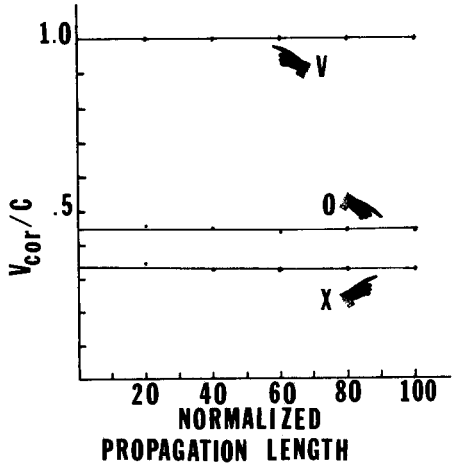

Fig. 10. Correlation velocity of 50-cycle wave packets propagating in vacuum and in the ordinary and extraordinary modes (perpendicular to the static magnetic field). $\omega_p/\omega_0 = 0.9$, $\nu/\omega_0 = 0.001$, and $\omega_c/\omega_0 = 0.09$. Data taken from Table II and Figs. 5 and 9. V—Vacuum propagation; O—ordinary wave; X—extraordinary wave.

where $k_{l,r}(\omega)$ is the propagation factor, and the upper sign refers to the left circularly polarized wave for $k_l(\omega)$ and the lower sign refers to the right circularly polarized wave for $k_r(\omega)$; the right circularly polarized wave rotates in the same sense as the electrons rotate. In the absence of collisions there is a resonance for $k_r(\omega)$ at the electron cyclotron frequency.

Two rather interesting features of Eq. (12) deserve mention. First, when the left and right circularly polarized wave packets mostly overlap, there is Faraday rotation of the plane of polarization due to the difference in phase velocity of the two modes. As a consequence of the $\mathbf{v} \times \mathbf{B}_0$ force the direction of rotation is the same whether the wave packet propagates parallel or antiparallel to $\mathbf{B}_0$; i.e., the polarization does not "unscrew" when the direction of propagation is reversed. Because of the difference in absorption of the two modes the total wave packet rapidly becomes elliptically polarized in the plane perpendicular to $\mathbf{B}_0$. Second, for large values of plasma frequency and cyclotron frequency the so-called whistler mode can propagate; in solid state physics, waves in this mode are known as helicons. The whistler mode was named for the descending whistle which is heard in the VLF part of the spectrum when such waves are initiated by lightning strokes

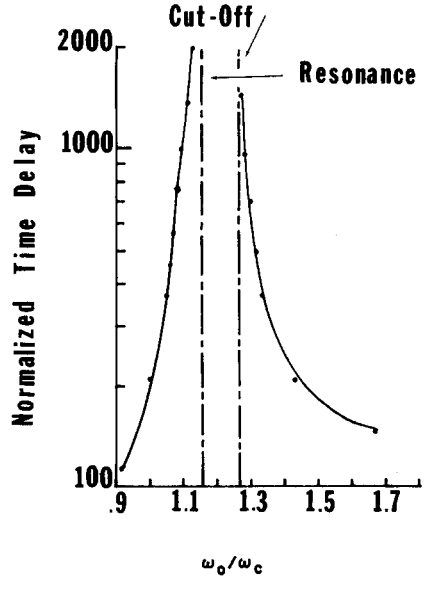

Fig. 11. Normalized time delay (in 4096 time) of extraordinary wave for ω_0 sweep through upper hybrid resonance. Cutoff occurs for $\omega_p/\omega_0 = 0.456851$ and $\omega_c/\omega_0 = 0.791289$. Resonance occurs for $\omega_p/\omega_0 = 0.5$ and $\omega_c/\omega_0 = 0.866025$. Without collisions there would be no propagation for Fourier components between cutoff and resonance. At upper hybrid resonance, $d/\lambda_0 = 100$ and $\nu/\omega_0 = 0.001$.

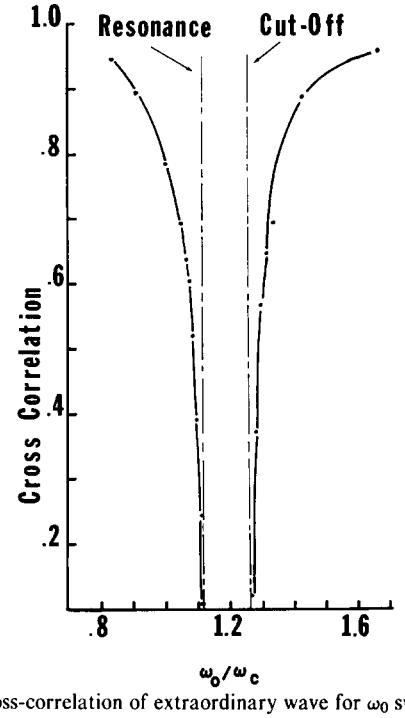

Fig. 12. Cross-correlation of extraordinary wave for ω_0 sweep through upper hybrid resonance, for same conditions as in Fig. 11.

or nuclear explosions. Actually, two values of ω_c/ω_0 exist for a given group velocity, so that the spectrum analysis of the received whistler shows a characteristic "nose" when plotted as a function of time.[44]

In Fig. 13 we plot the x component of the wave packet as it propagates along the magnetic field. The coordinate system is such that the original pulse is polarized along the x axis and $\mathbf{B}_0$ is along the z axis. The y component is plotted in Fig. 14. One observes the decrease of the x component and the growth of the y component. The cross-correlations for this case are plotted in Figs. 15 and 16, and it is apparent that the x component decorrelates due to rotation as well as dispersion and absorption. The increasing correlation of the y component is due to rotation dominating the effects of dispersion and absorption. For Figs. 13–16 the Faraday rotation and ellipticity of the central frequency of the original pulse are shown in Table III.

In Fig. 17 we show the separation of a linearly polarized pulse into two circularly polarized wave packets, and Fig. 18 shows the cross-correlations. The faster wave packet is left circularly polarized; the slower is right circularly polarized. The resolution of the pulse into two wave packets is much more clear in the cross-correlation than in the waveform itself. The right circularly polarized packet suffers more absorption than the left because the right rotates in the same sense as the electrons.

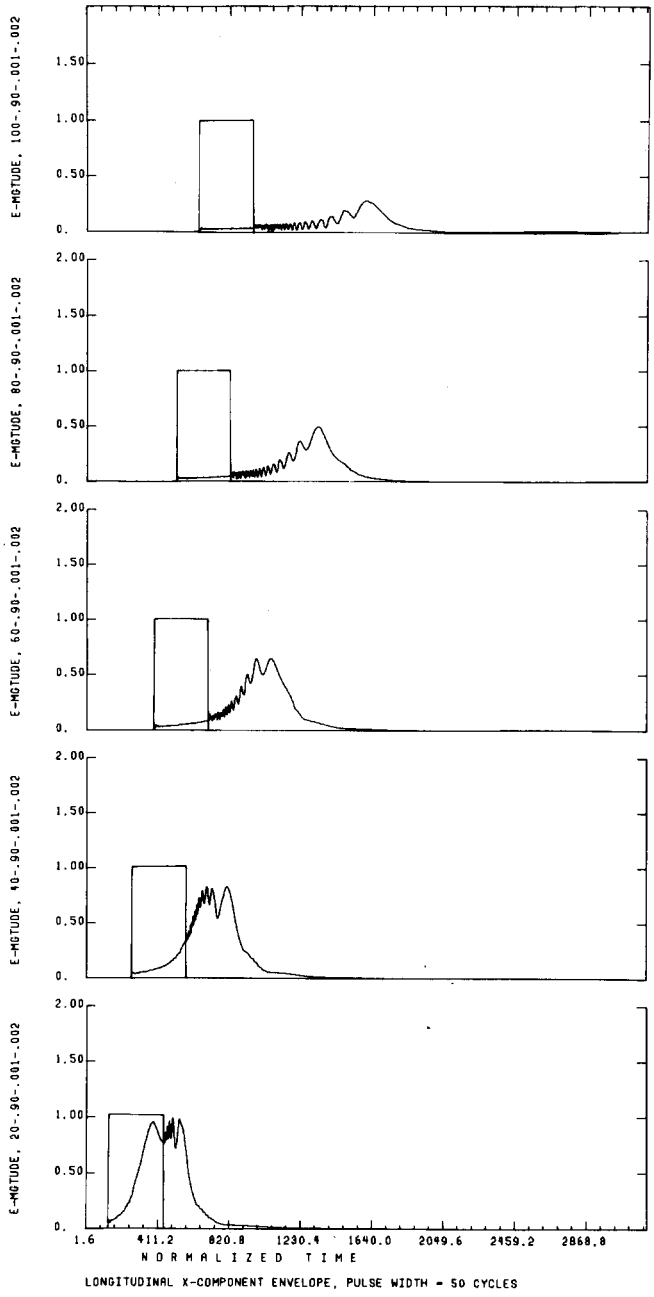

Fig. 13. x component of waveform for longitudinal propagation. $\omega_p/\omega_0 = 0.9$, $\nu/\omega_0 = 0.001$, $\omega_c/\omega_0 = 0.002$, and pulse width = 50 cycles. Note decrease of x component, partly due to absorption but mostly due to rotation.

In Fig. 19 we plot the time delay of the maximum cross-correlation as a function of $(\omega_c/\omega_0)^{-1}$. The inverse of the normalized cyclotron frequency was chosen for the abscissa for scale convenience and to permit comparison

Table III. Normalized time delay and cross-correlation for propagation parallel to $\mathbf{B}_0$. $\omega_p/\omega_0 = 0.9$, $\nu/\omega_0 = 0.001$, $\omega_c/\omega_0 = 0.002$, pulse width = 50 cycles.

d/λ_0	y component 4096 time	x component 4096 time	Maximum y cross-correlation	Maximum x cross-correlation	Faraday rotation[a]	Ellipticity[a]
20	372	354	0.18632	0.78187	13.3786	0.0010
40	725	723	0.31220	0.61830	26.7573	0.0019
60	1103	1109	0.40749	0.48117	40.1359	0.0029
80	1457	1455	0.43387	0.32444	53.5146	0.0039
100	1835	1765	0.41109	0.17861	66.8932	0.0048

[a] Faraday rotation (in degrees) and ellipticity computed for ω_0.

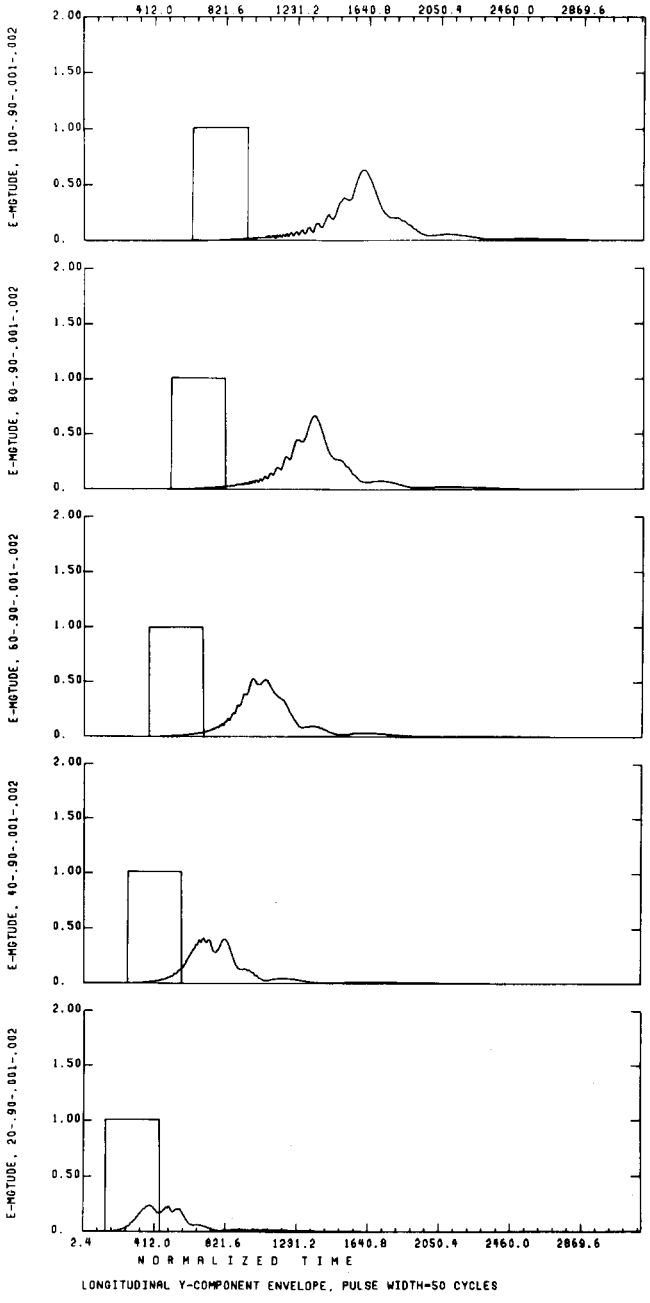

Fig. 14. y component of waveform for longitudinal propagation for same conditions as in Fig. 13.

with group velocity results of Vidmar and Crawford.[45] The high-speed Fourier components comprising the "nose" of the whistler are very evident. The high-frequency branch is observed with scans of wide bandwidth in the ionosphere, but since the lower frequency branch lies in the audible region, the received signal was described in early papers as having a chirp with a descending frequency.

IV. SUMMARY AND CONCLUSIONS

We have shown that the correlation velocity provides a reliable measure of the velocity of a wave packet in a dispersive, absorptive medium, with nonreciprocal anisotropy. The correlation velocity is explicitly defined in terms of length/time, and overcomes many of the objections to previously suggested measures of velocity. All of the computations here have been for a sinusoidal wave with a rectangular pulse envelope of fixed width. This is a very common waveform, such as might be used by students in a lab or field experiment; it is also the fundamental waveform of simple radars and binary-coded communications. Bats, dolphins, killer whales, and sophisticated radars and sonars use more complicated waveforms. The question naturally arises concerning the combined effects of waveform (or spectrum), in a particular dispersive situation, on the correlation velocity. This is a topic of considerable interest; the coding of waveforms to attain specific objectives in terms of cross-correlations is under active study. In radar, for example, one is faced with two-dimensional cross-correlation functions in a time–frequency space, and it is often required to move the distribution of the cross-correlation function about. In underwater sound propagation where the dispersion relation is often well known some success has been achieved in designing "matched signals" instead of

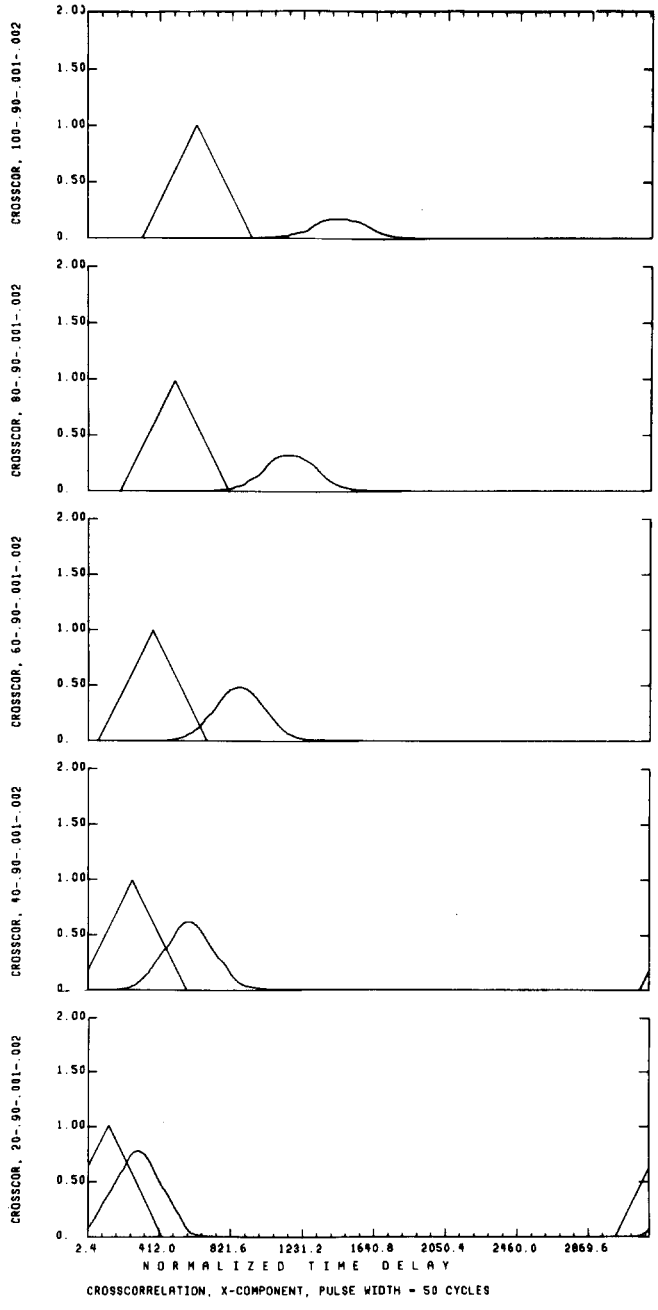

Fig. 15. Cross-correlation of original signal and received x component for same conditions as in Fig. 13. (See Table III for data.)

"matched filters."[1] Some of the effects of pulse width (spectrum width) can be seen in Figs. 3 and 4 of Ref. 35, in which the particular dispersive situation produces a slightly greater velocity as the pulse width decreases (as the spectrum width increases). For this case the slower, lower frequencies are diminished relative to the faster high frequencies, resulting in a speedier arrival of the pulse.

Why do we need to define a velocity, since it may be slightly dependent on pulse shape? First, we often need to determine transmission path length by $d = "v"t$ in situations where we can calibrate or compensate for pulse shape effects; second, we are often interested in changes in "v" for a fixed path in order to relate this to changes in the medium. As an example, we have shown in Figs. 6 and 7 how the fine details of the dispersive effect of absorption,[22] manifested here as a small increase in v_{cor}, can be extracted from the

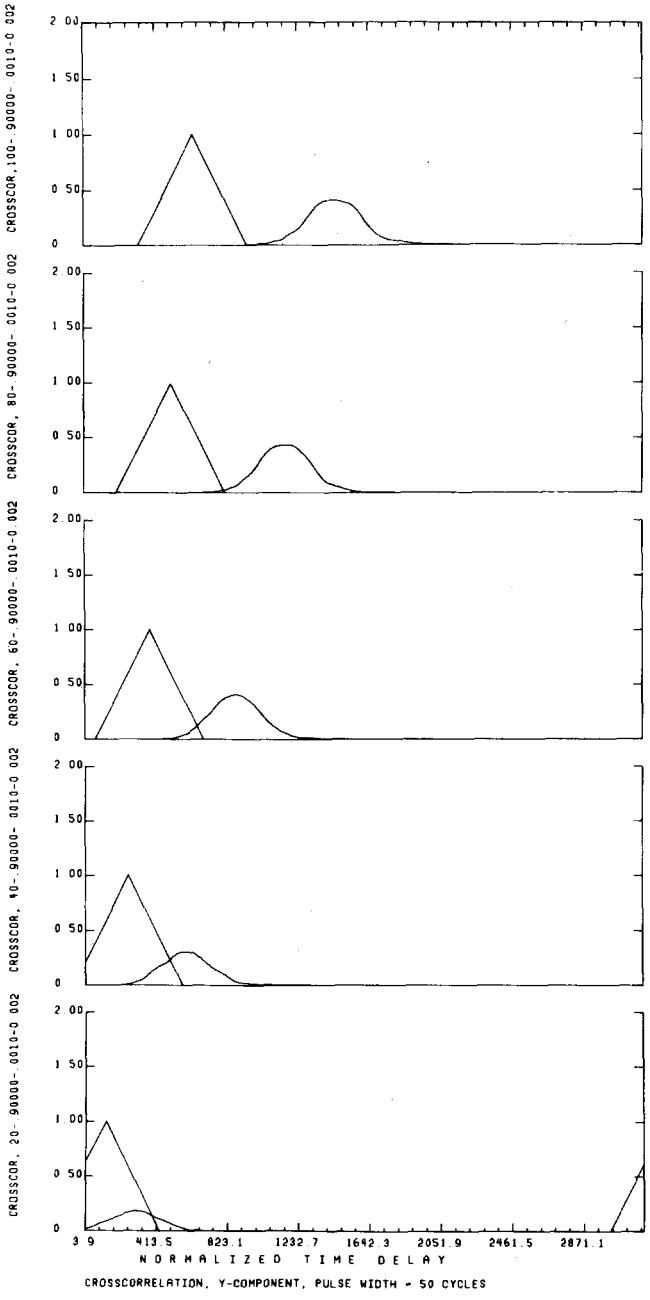

Fig. 16. Cross-correlation of original signal and received y component for same conditions as in Fig. 14. (See Table III for data.)

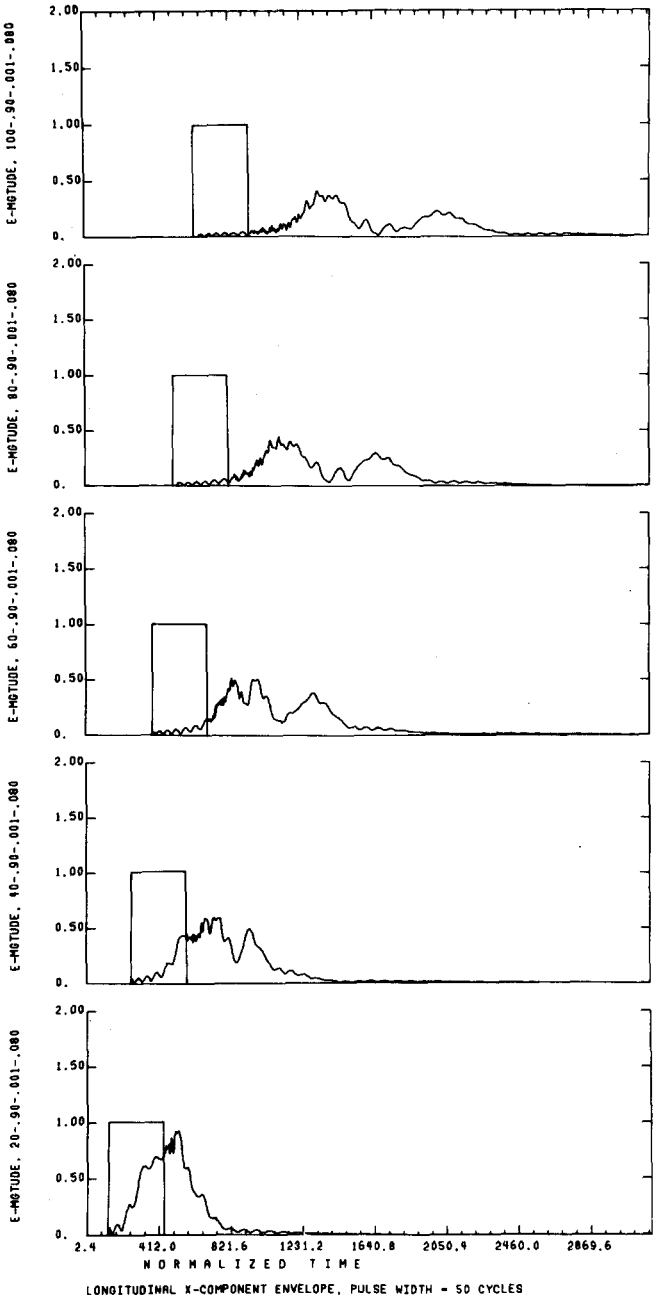

Fig. 17. Separation of x component into left and right circularly polarized wave forms, for longitudinal propagation. $\omega_p/\omega_0 = 0.9$, $\nu/\omega_0 = 0.001$, $\omega_c/\omega_0 = 0.08$, and pulse width = 50 cycles. Left circularly polarized part arrives first.

cross-correlation function although it is obscured in the waveform itself.

We have also shown that the correlation velocity has high immunity to noise and natural fluctuations of the medium which tend to introduce error into previously used velocities. For example, consider the centrovelocity in the presence of noise and statistical fluctuations represented by a random field $\mathbf{E}_r(\mathbf{r},t)$, as in Eqs. (5)–(8). Since the total field at the detector is now $\mathbf{E}(\mathbf{r},t) + \mathbf{E}_r(\mathbf{r},t)$, the centrovelocity given by Eq. (1) becomes

$$v_c = \left| \nabla \left[\left(\int_{-\infty}^{+\infty} t[\mathbf{E}(\mathbf{r},t) + \mathbf{E}_r(\mathbf{r},t)]^2 \, dt \right) \times \left(\int_{-\infty}^{+\infty} [\mathbf{E}(\mathbf{r},t) + \mathbf{E}_r(\mathbf{r},t)]^2 \, dt \right)^{-1} \right] \right|^{-1}. \quad (13)$$

In Eq. (13) one sees that v_c would be generally biased by the presence of noise, resulting in a different value than it would achieve in the ideal noise-free case. Signal averaging prior to computation with Eq. (13) would, of course, be beneficial but signal averaging would enhance the correlation velocity even more if it were done before use in Eq. (2) or (3). As an extreme example one might obtain a value for v_c even in the absence of a signal, using Eq. (13). Furthermore, signal averaging has no meaning for a single event; Tolstoy shows an actual case in which not only the time of arrival of a seismic pulse thought to originate at an underground explosion, but its very existence, was determined by cross-correlating a signal plus noise with a replica of an anticipated waveform (in this case, a chirp).[46]

In cases where pulse stretching and pulse repetition rate are such that the trailing edge of a pulse overlaps the leading

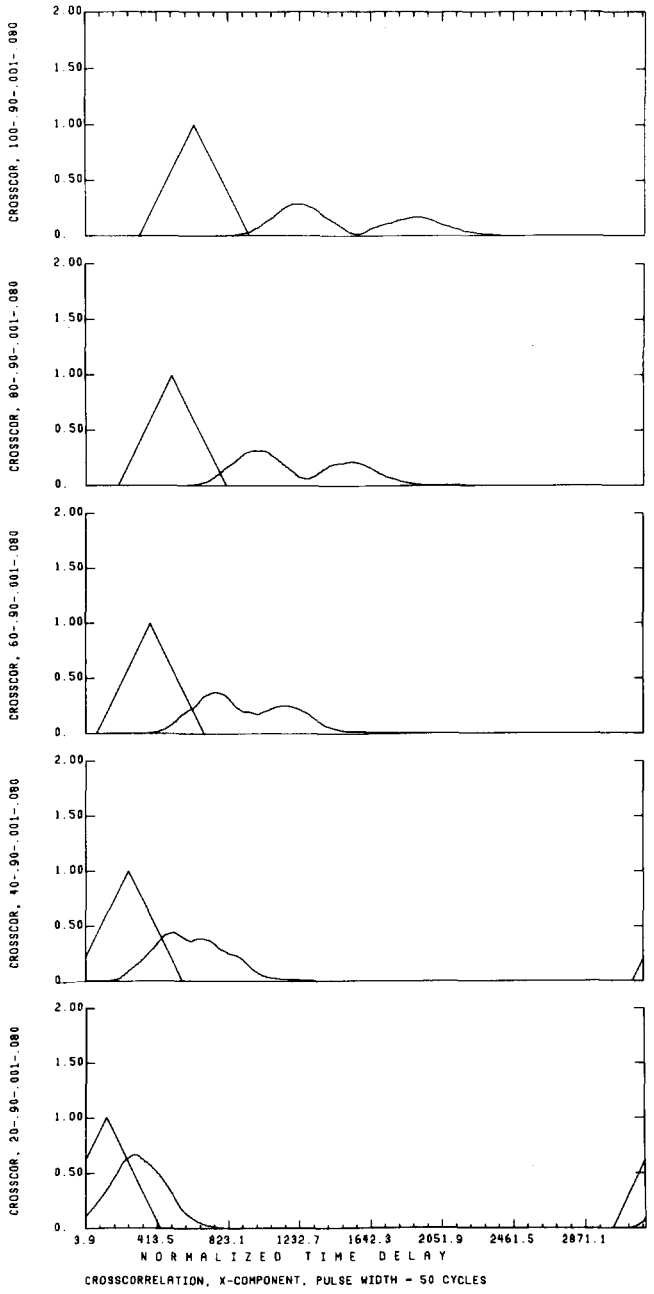

Fig. 18. Cross-correlation of original signal and received x component for same conditions as in Fig. 17. Note how separation into two wave packets is more apparent in cross-correlation than in waveform.

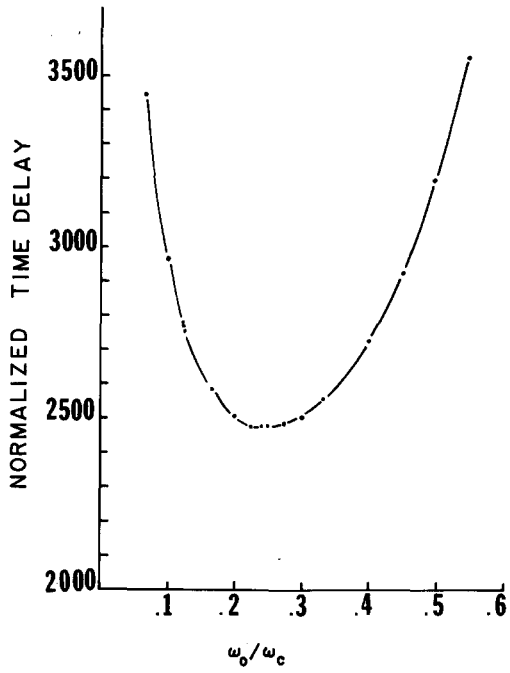

Fig. 19. Normalized time delay (in 4096 time) of maximum cross-correlation for whistler mode propagation. Note slow speed of this mode relative to previous examples. $d/\lambda_0 = 20$, $\nu/\omega_0 = 0.0005$, and pulse width = 50 cycles. In this curve we hold ω_0 fixed and vary ω_p and ω_c, keeping the ratio $\omega_p/\omega_c = 10$. Maximum velocity (minimum delay) occurs for $\omega_c/\omega_0 = 4$. To obtain the time-varying spectrum similar to that in Ref. 44, this figure should be reflected in a plane containing the horizontal axis, perpendicular to the paper, and the reflected image should then be rotated 90° counterclockwise.

edge of another pulse, signal averaging for the centrovelocity is of help only in removing noise. Correlation velocity, on the other hand, is relatively unaffected by pulse overlap. This effect can be seen in some of the previous figures.

It is intuitively clear that there is a close connection between the correlation receiver that we have discussed here and the matched filter that we have discussed earlier.[1] In fact, a cross-correlation system is often an optimum realization of a matched filter. A large computer is no longer necessary; a digital-processing oscilloscope makes an acceptable correlation receiver.[47] Remarkably, a single integrated circuit that will perform cross-correlation has just been introduced,[48] opening up interesting possibilities for inexpensive student experiments.[49]

Finally, there are two other practical aspects of the current interest in dispersive propagation. Very high rates of information transmission require very short pulses associated with such broad spectra that they almost always encounter dispersion. Also, very short pulses have such a low spectral energy density that they are hard to find unless you know what to look for (hence, cross-correlation). A pulse of 1 nsec, pulsed a thousand times per second, is on for less than 32 sec per year, and a 1-psec pulse is almost never there!

ACKNOWLEDGMENTS

I wish to thank P. W. Lyons for his excellent assistance in computer programming for this work, and Professor N. L. Oleson for his helpful suggestions and comments. This work was supported in part by GTE Laboratories, Inc.

[1]S. C. Bloch, Am. J. Phys. **41,** 857 (1973). [Here we attributed the basic idea of chirp radar to another person; R. H. Dicke (private communication) has informed us of his priority in this invention documented in a patent application.]
[2]W. C. Elmore and M. A. Heald, *The Physics of Waves* (McGraw-Hill, New York, 1969), pp. 431–435.
[3]J. D. Jackson, *Classical Electrodynamics,* 2nd ed. (Wiley, New York, 1975), pp. 299–306, 313–326.
[4]J. A. Stratton, *Electromagnetic Theory* (McGraw-Hill, New York, 1941), pp. 301–309.
[5]L. Brillouin, *Wave Propagation and Group Velocity* (Academic, New York, 1960). [Incidentally, anyone who has ever questioned the wisdom of the committee that decides Nobel prizes should read the Foreword to this book in regard to Sommerfeld.]
[6]F. S. Crawford, Jr., Am. J. Phys. **38,** 378 (1970).
[7]F. S. Crawford, Jr., Am. J. Phys. **38,** 1477 (1970).
[8]F. S. Crawford, Jr., Am. J. Phys. **39,** 610 (1971).
[9]J. R. Merrill, Am. J. Phys. **39,** 539 (1971).
[10]S. Aksornkitti, H. C. S. Hsuan, and K. E. Lonngren, Am. J. Phys. **37,** 783 (1969).
[11]K. E. Lonngren, W. F. Ames, H. C. S. Hsuan, I. Alexeff, and W. Wing, Am. J. Phys. **40,** 484 (1972).
[12]I. Alexeff, Am. J. Phys. **40,** 763 (1972).
[13]D.L. Landt, C. M. Burde, H. C. S. Hsuan, and K. E. Lonngren, Am. J. Phys. **40,** 1493 (1972).
[14]D. York, Am. J. Phys. **43,** 725 (1975).
[15]L. C. Baird, Am. J. Phys. **40,** 327 (1972).
[16]W. V. Prestwich, Am. J. Phys. **43,** 832 (1975).
[17]J. Jones, Am. J. Phys. **42,** 43 (1974).
[18]M. V. Berry and D. A. Greenwood, Am. J. Phys. **43,** 91 (1975).
[19]E. A. Guillemin, *Introductory Circuit Theory* (Wiley, New York, 1953), pp. 270–273.
[20]W. P. Healy and E. A. Power, Am. J. Phys. **42,** 1070 (1974).
[21]C. Dean, Am. J. Phys. **41,** 1283 (1973).
[22]D. Rader, Am. J. Phys. **41,** 420 (1973). Also see R. A. Fisher, *ibid.* **44,** 1002 (1976) and D. Rader, *ibid.* **44,** 1005 (1976).
[23]R. W. Christy, Am. J. Phys. **40,** 1403 (1972).
[24]D. C. Khan and A. Mahendra, Am. J. Phys. **38,** 1258 (1970).
[25]C. H. Holbrow and W. C. Davidon, Am. J. Phys. **32,** 762 (1964).
[26]M. Sharnoff, Am. J. Phys. **32,** 40 (1964).
[27]A. Scott, Am. J. Phys. **32,** 713 (1964).
[28]K. Suchy, Proc. IEEE **62,** 1571 (1974).
[29]J. A. Bennett, Proc. IEEE **62,** 1577 (1974).
[30]K. A. Connor and L. B. Felsen, Proc. IEEE **62,** 1586 (1974).
[31]D. G. Anderson and J. I. H. Askne, Proc. IEEE **62,** 1518 (1974).
[32]D. G. Anderson, J. I. H. Askne, and M. Lisak, Proc. IEEE **63,** 715 (1975).
[33]R. Buckley, J. Plasma Phys. **13,** 539 (1975).
[34]C. E. Seyler, Jr., S. C. Bloch, and R. W. Flynn, J. Geophys. Res. **77,** 4237 (1972).
[35]S. C. Bloch, A. P. Boss, and P. W. Lyons, J. Geophys. Res. **79,** 5261 (1974).
[36]S. C. Bloch and P. W. Lyons, Proc. IEEE **64,** 224 (1976).
[37]H. S. Robertson, Q. J. Fl. Acad. Sci. **34,** 93 (1971).
[38]R. L. Smith, Am. J. Phys. **38,** 978 (1970).
[39]W. K. H. Panofsky and M. Phillips, *Classical Electricity and Magnetism,* 2nd ed. (Addison-Wesley, Reading, MA, 1962), pp. 413–414.
[40]H. Kroemer, Proc. IEEE **63,** 988 (1975); J. N. Churchill, *ibid.* **65,** 489 (1977).
[41]G. Russakoff, Am. J. Phys. **38,** 1188 (1970). (Also see Ref. 3, pp. 226–241.)
[42]Reference 39, pp. 8, 28–40.
[43]S. C. Bloch, Phys. Rev. **144,** 181 (1966).
[44]D. L. Carpenter, J. Geophys. Res. **71,** 693 (1966).
[45]R. J. Vidmar and F. W. Crawford, in *Proceedings of the XIIth International Conference on Phenomena in Ionized Gases,* Eindhoven, The Netherlands, August 1975 (North-Holland, Amsterdam, 1975), p. 316.
[46]I. Tolstoy, *Wave Propagation* (McGraw-Hill, New York, 1973), p. 385.
[47]*Tektronix Handshake,* No. 3, p. 4 (1976).
[48]Integrated circuits TAD-32, BAC-32, or AAC-32, available from Reticon Corp., Sunnyvale, CA 94086.
[49]Additional practical applications can be found in Technical Bulletin 14 (Signal Analysis Industries Corp., Hauppauge, NY 11787); Monograph No. 1 (Federal Scientific Corp., New York, NY 10027); P. J. Garforth, Electr. Instrum. Dig. **6** (8), 7 (1970). An interesting example of a correlation receiver built by the Norwegian Defence Research Establishment is shown in: C. W. Horton, Sr., *Signal Processing of Underwater Acoustic Waves* (U.S. GPO, Washington, DC), pp. 172–173.